Electronic Supplementary Material (ESI) for Materials Advances.

Appendix

Supplementary figures

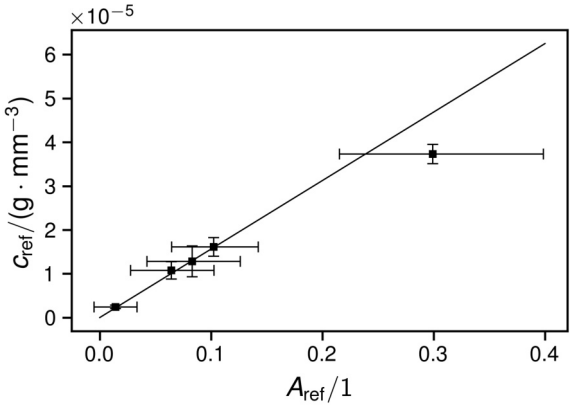

Figure S1: Relation of the absorbance A_{ref} to the BCB concentration. The regression line represents $c_{\text{ref}} = A_{\text{ref}}/(\epsilon\, l)$ from which ϵ could be obtained as ϵ = (1.30$\pm$0.27)·10^5 mm^2 g^{-1}.

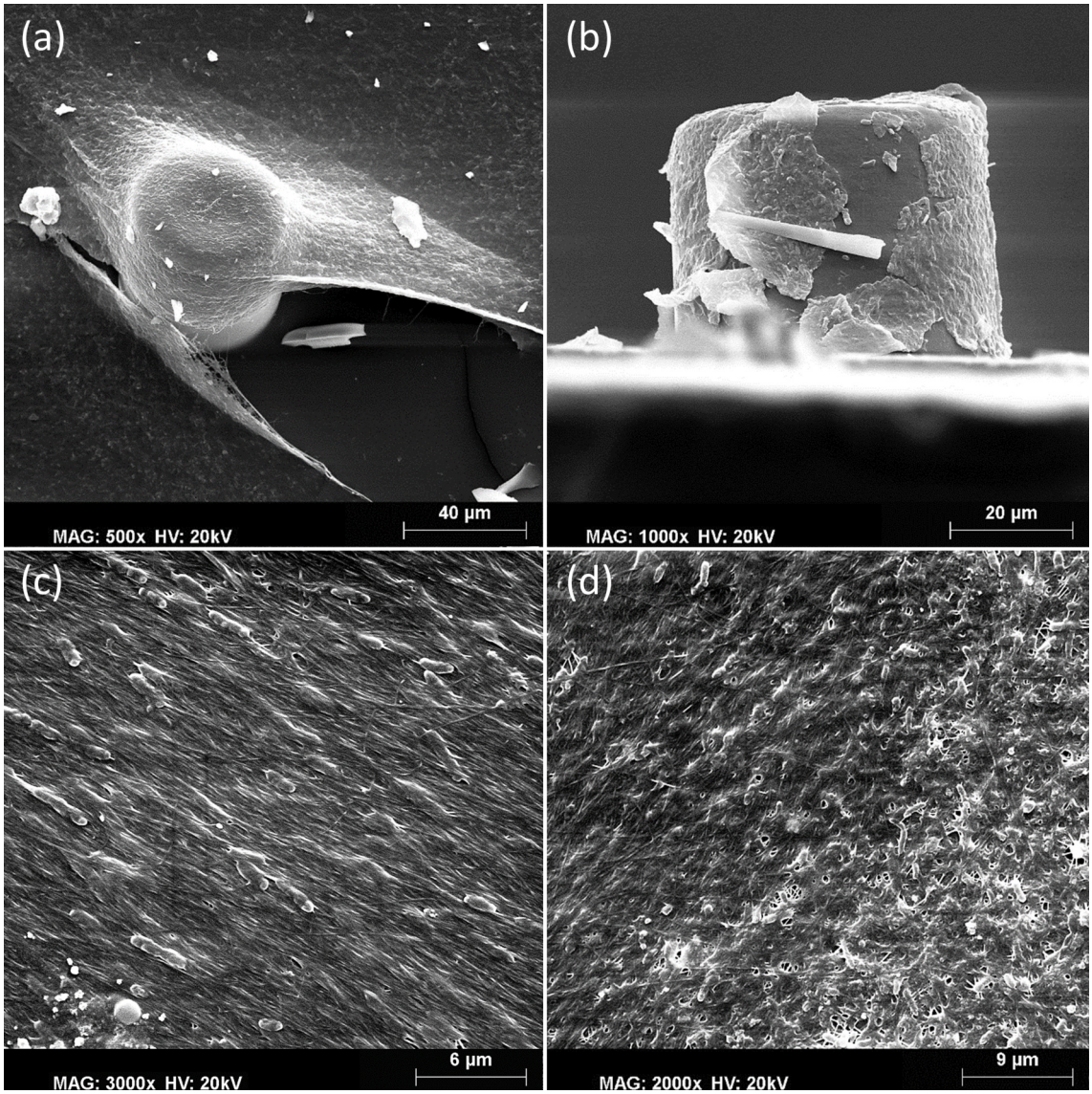

Figure S2: SEM micrographs of the BCB with (a) and (b) showing an obstacle covered by BCB. In (c) the fiber orientation is visible. Image (d) shows the difference between the thicker streamers (right) and the thinner film (left). Between the fibers *K. xylinus* can be observed as with its 2-4 µm length and 0.5 - 1 µm thickness.

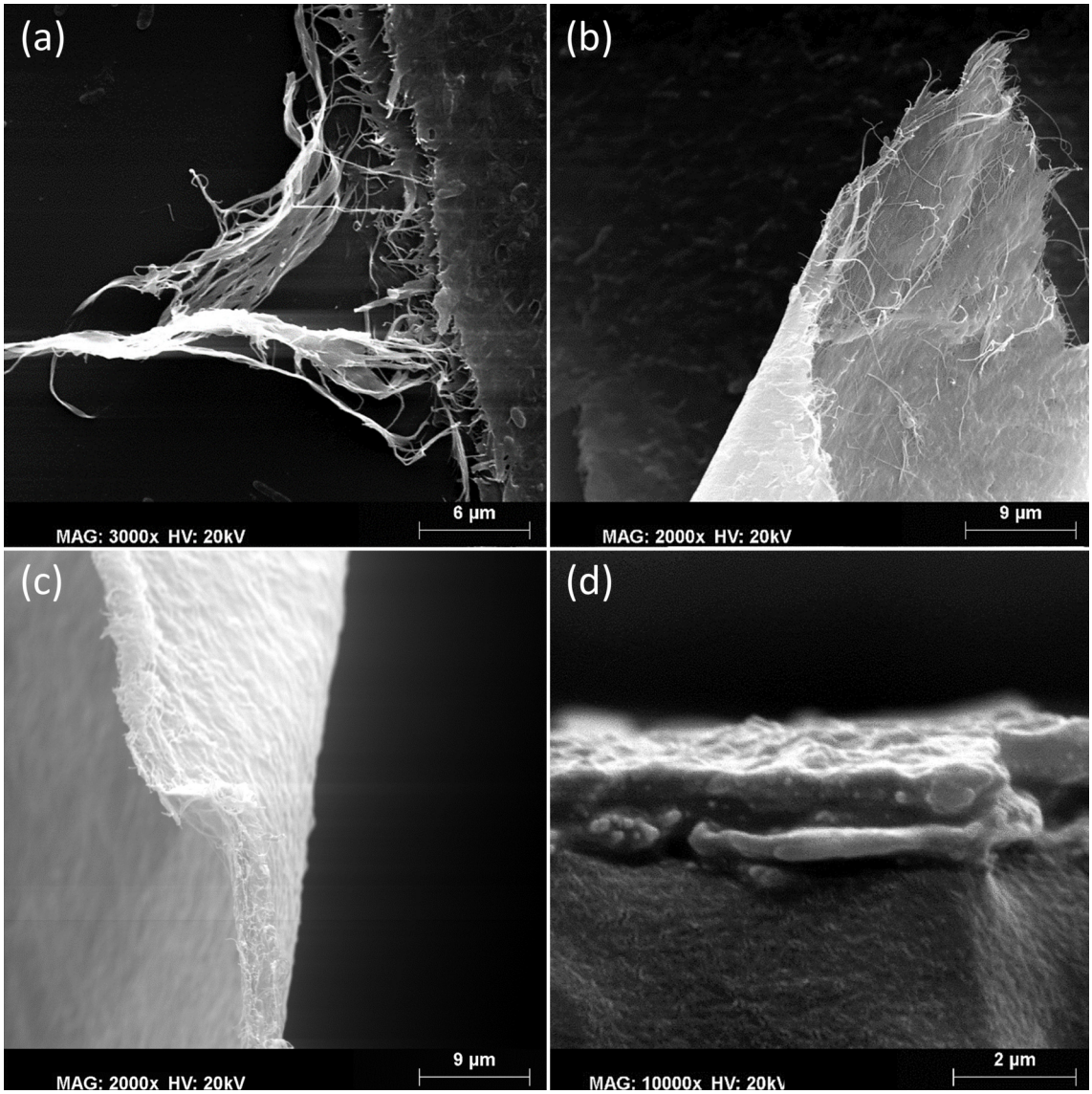

Figure S3: SEM micrographs of the BCB edge. In (a) the multilayered texture can be seen from above, with image (b) showing one of theses layers. The topviewed layer in (c) is frayed after tearing, making the measurement of the thickness difficult. After freezing and breaking of the BCB the packed cross section could be obtained without fraying, image (d). This image was one used in the BCB concentration calibration steps.

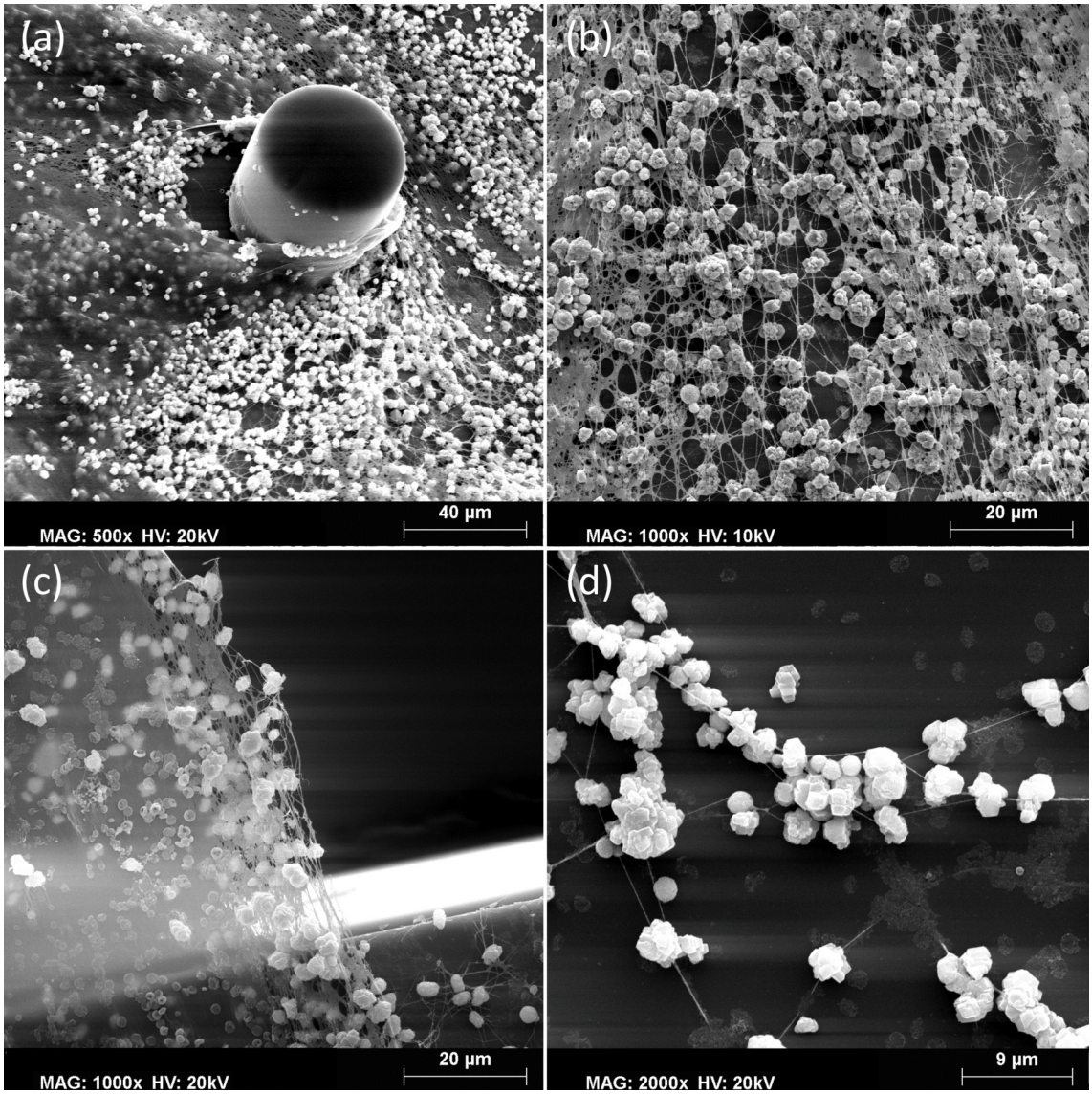

Figure S4: SEM micrographs of the $CaCO_3$ mineralised BCB. The $CaCO_3$ phases are embedded in the BC fiber networks.

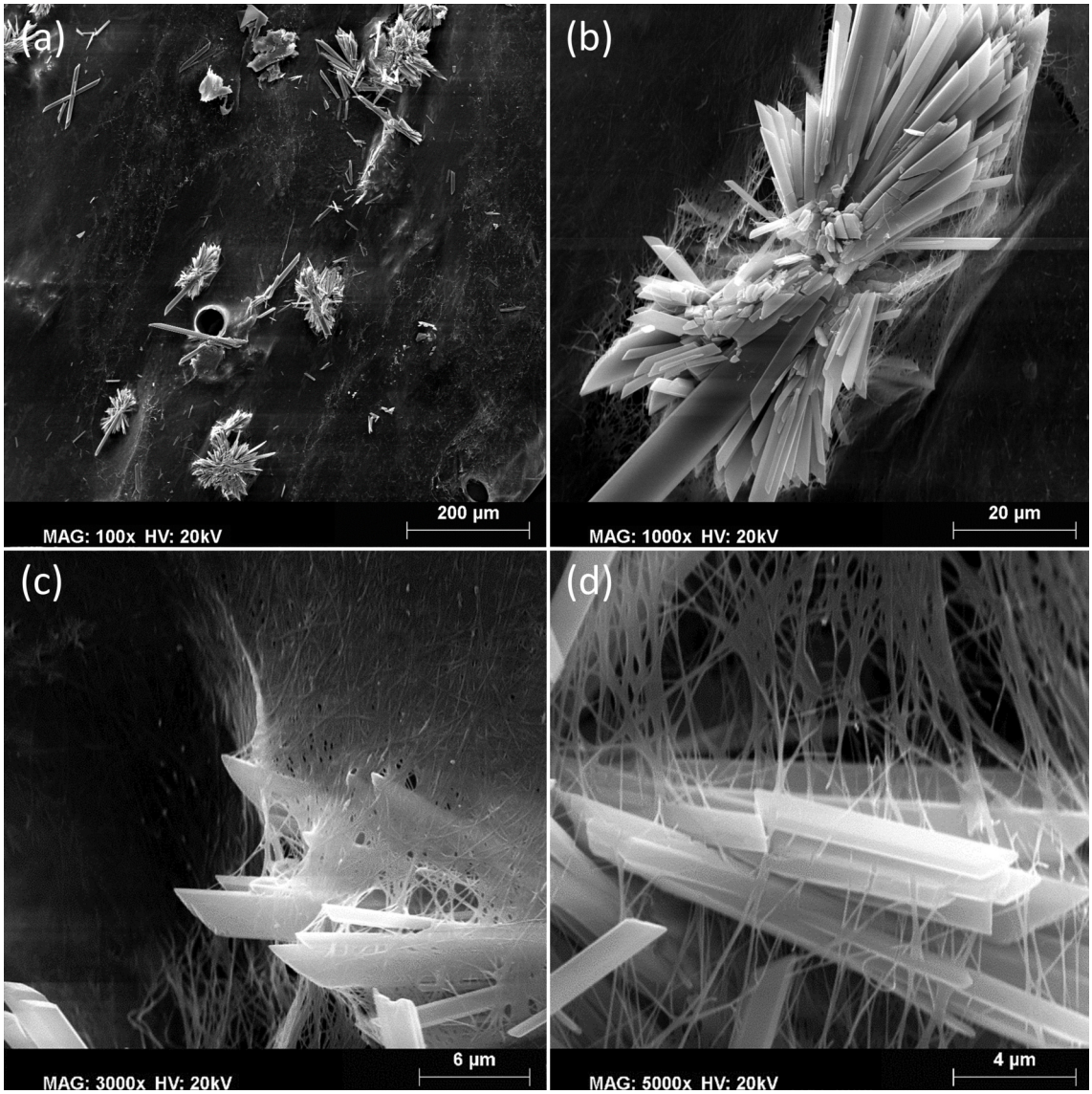

Figure S5: SEM micrographs of the gypsum mineralised BCB. The spatial spread gypsum aggregates (a) tended to grow slightly oval, apparently with no regard to the BCB (b). A closer look on the long side of the oval showing crystallites interact with the BC network, which here is preferred perpendicular oriented (c, d).

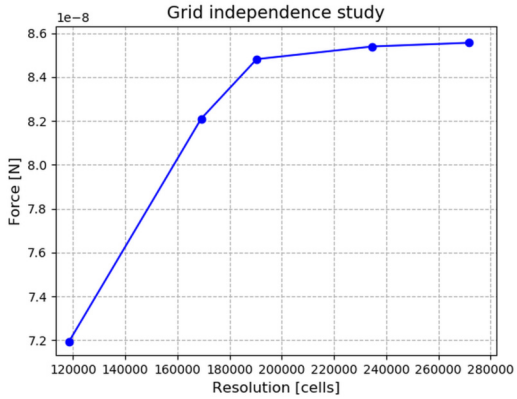

Figure S6: A graphical independence study was performed using, five different resolved meshes: very coarse (118347 cells), coarse (169108 cells), medium (190370 cells), fine (234714 cells) and extra fine (271818 cells). The simulation showed that the difference of the force on the last four separators of the inlet. It was 2.79 % between the coarse and the extra fine mesh, 0.74 % between the medium and extra fine mesh and 0.16 % between the fine and the extra fine mesh. It is therefore evident that from the fine mesh onwards there are no longer any significant changes of the result.

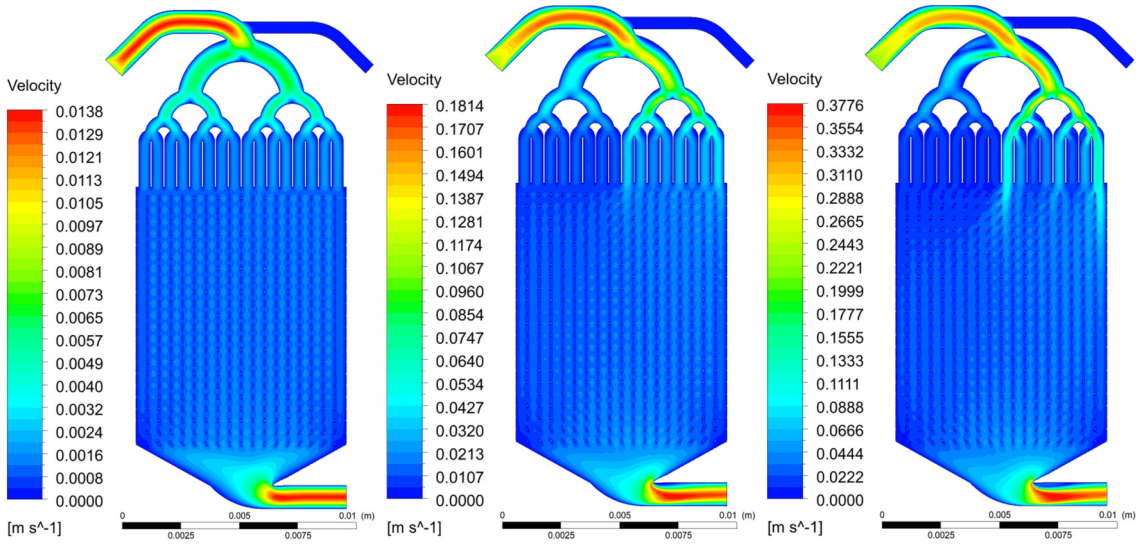

Figure S7: Contour plots of the microfluidic cell at the flow rates 1.0 mm s^{-1} (left), 12.5 mm s^{-1} (middle) and 25.0 mm s^{-1} (right)

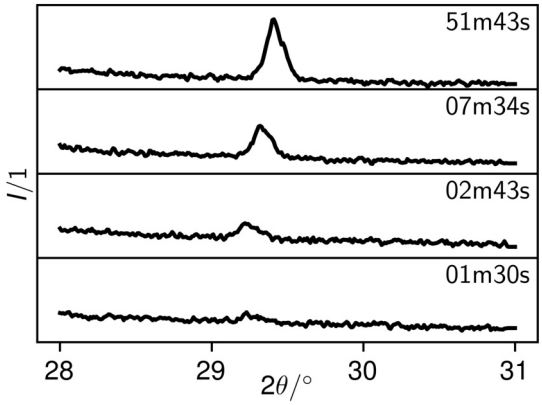

Figure S8: XRD data of the crystallization of ACC as calcite: Development of the (104) reflex. The slight displacement of the reflex results from the crystal displacement by sinking down in the sample holder during their formation.

Supplementary video

Figure S9: Growth of BCB in the microfluidic PDMS cell at a flow rate of 1.0 mm s^{-1}.